Digital Signal Processing 23 (2013) 780–790

Contents lists available at SciVerse ScienceDirect

Digital Signal Processing

www.elsevier.com/locate/dsp

A time–frequency based approach for generalized phase synchrony assessment in nonstationary multivariate signals

Amir Omidvarnia [a,*], Ghasem Azemi [a,b], Paul B. Colditz [a], Boualem Boashash [a,c]

[a] University of Queensland Centre for Clinical Research, RBWH, Herston, QLD 4029, The University of Queensland, Brisbane, Australia
[b] Department of Electrical Engineering, Razi University, Kermanshash, Iran
[c] Qatar University College of Engineering, Doha, Qatar

ARTICLE INFO

Article history:
Available online 9 January 2013

Keywords:
Phase synchrony
Instantaneous frequency
Cointegration
Newborn EEG
Time–frequency analysis

ABSTRACT

This paper proposes a new approach to estimate the phase synchrony among nonstationary multivariate signals using the linear relationships between their instantaneous frequency (IF) laws. For cases where nonstationary signals are multi-component, a decomposition method like multi-channel empirical mode decomposition (MEMD) is used to simultaneously decompose the multi-channel signals into their intrinsic mode functions (IMFs). We then apply the Johansen method on the IF laws to assess the phase synchrony within multivariate nonstationary signals. The proposed approach is validated first using multi-channel synthetic signals. The method is then used for quantifying the inter-hemispheric EEG asynchrony during ictal and inter-ictal periods using a newborn EEG seizure/non-seizure database of five subjects. For this application, pair-wise phase synchrony measures may not be able to account for phase interactions between multiple channels. Furthermore, the classical definition of phase synchrony, which is based on the rational relationships between phases, may not reveal the hidden phase interdependencies caused by irrational long-run relationships. We evaluate the performance of the proposed method using the differentiation of unwrapped phase as well as other IF estimation techniques. The results obtained on newborn EEG signals confirm that the generalized phase synchrony within EEG channels increases significantly during ictal periods. A statistically consistent phase coupling is also observed within the non-seizure segments supporting the concept of constant inter-hemispheric connectivity in the newborn brain during inter-ictal periods.

1. Introduction

Phase synchrony has been used to investigate the dynamics of complex systems which result from time-varying interactions of several subsystems. The human brain is a complex system with different components interacting with each other dynamically. Pair-wise phase synchrony is quantified using bivariate measures. However, pair-wise measures of single channels do not necessarily lead to a complete picture of the global interactions within a nonstationary multi-channel signal (such as EEG) and nor does multivariable analysis [1].

The concept of analytic signals [2,3] and complex Gabor wavelet filtering [4] are usually utilized to extract the instantaneous phase of a real-valued signal. A measure of phase synchrony is then computed from the resulting phase information [4]. Several methods were proposed for the evaluation of phase synchrony for bivariate and multivariate signals including *Mean Phase Coherence* (also, sometimes referred to as *Phase-Locking Value*) [3,4], *Evolution Map Approach* [5], *Instantaneous Period Approach* [6], *Mutual Prediction Approach* [6], *General Field Synchronization* [7], empirical mode decomposition (EMD) based methods [8,9] and *frequency flows analysis* [10]. All of these methods are restricted by the assumption that the phase-locking ratio between signals is always rational. This restriction has been lately relaxed by proposing a generalized version using the concept of *cointegration* [11,12] where the phase-locking ratio is allowed to be irrational. Such generalization covers the classical definition as a special case, while it shares a broader view of phase interactions which can be observed in neuronal signals [13].

To address the above, this paper proposes a novel approach for extracting generalized phase synchronicity for nonstationary multivariate signals, based on an interpretation of the generalized phase synchrony (GePS) using the linear relationship between instantaneous frequency (IF) laws. The proposed method is evaluated using several IF estimators on a simulated dataset as well as a multi-channel newborn EEG seizure/non-seizure database of five subjects.

* Corresponding author. Fax: +61 7 3346 5509.
E-mail addresses: a.omidvarnia@uq.edu.au (A. Omidvarnia), g.azemi@uq.edu.au (G. Azemi), p.colditz@uq.edu.au (P.B. Colditz), boualem@qu.edu.qa (B. Boashash).

1051-2004/$ – see front matter
http://dx.doi.org/10.1016/j.dsp.2013.01.002

Table 1
Time-lag kernels of the TFDs and their parameters utilized in this study. The parameters N, L_w and L_{lag} denote the time length of the segment in samples, the window function length and the lag window length, respectively.

TFD	Discrete form of the time-lag kernel $G[n,m]$	Parameter(s)
SPEC	$w[n+m]w[n-m]$	Rectangular window w ($L_w = N/4$)
MBD	$\frac{\cosh^{-2\beta} n}{\sum_{n=1}^{N} \cosh^{-2\beta} n}$	$\beta = 0.01$, $L_{lag} = N/4$
CWD	$\frac{\sqrt{\pi\sigma}}{2\lvert m\rvert} e^{-\pi^2\sigma n^2/4m^2}$	$\sigma = 10$, $L_{lag} = N/4$

The remainder of the paper is organized as follows: Section 2 provides a brief review of relevant time–frequency (T-F) signal analysis and covers quadratic T-F distributions (QTFDs), EMD and IF estimators. Section 3 explains the concept of bivariate phase synchrony and its extension to GePS using the concept of cointegration. Section 4 introduces the proposed IF-based approach for GePS assessment. Section 5 presents and interprets the results obtained from the simulated data and newborn EEG datasets. Section 6 concludes the paper.

2. Time–frequency analysis and IF estimation: a brief review

T-F signal processing (TFSP) allows signal analysis in both time and frequency domains simultaneously and is therefore an effective tool for dealing with nonstationary signals [2].

2.1. Quadratic TFDs

Dealing with nonstationary signals whose frequency content changes over time is a common situation in many engineering areas including biomedical signal processing [6,14,15], radar [16–18] and telecommunications [19,20]. For the analysis of nonstationary signals, T-F distributions (TFDs) are the most suitable tools as they provide two-dimensional representations that reflect the time-varying spectral characteristics of the nonstationary signal and show how the energy of the signal is distributed over the two-dimensional T-F space. They also determine the number of signal components, the start and stop times and frequency range of an event in the signal. Quadratic TFDs (QTFDs) are the most commonly used TFDs and can be considered as smoothed versions of the Wigner–Ville Distribution (WVD) [2]. The discrete version of a QTFD with time-lag kernel $G[n,m]$ is given by [2]:

$$\rho_z[n,k] = 2 \underset{m\to k}{DFT}\left\{ G[n,m] \overset{*}{}_{n} \left(z_s[n+m] z_s^*[n-m] \right) \right\}, \quad k = 1,\ldots,M, \tag{1}$$

where * denotes the complex conjugation, the symbol $\overset{*}{}_{n}$ represents discrete convolution over time and $z_s[n]$ is the analytic associate of the real signal $s[n]$, $n = 0,\ldots,N-1$, i.e.,

$$z_s[n] = s[n] + jH\big(s[n]\big) = a_z[n] e^{j\varphi_z[n]}, \tag{2}$$

with $H(.)$ being the Hilbert transform operator. The resulting $\rho_z[n,k]$ is an $M \times N$ matrix where M is the number of frequency bins. In (2), $a_z[n]$ and $\varphi_z[n]$ are respectively the instantaneous amplitude and instantaneous phase (IP) of the signal. As reduced interface TFDs (RIDs) have been shown to be efficient in the analysis and processing of EEG signals [21–23], three popular RIDs; i.e. spectrogram (SPEC), modified-B distribution (MBD) and Choi–Williams distribution (CWD), are used in this study for IF estimation [2]. Our selection is also based on the comparison of TFDs in [24] where SPEC, MBD and CWD are ranked within the first four high-resolution TFDs. Table 1 summarizes the discrete forms of the time-lag kernels and their parameters utilized in this study.

2.2. Instantaneous frequency: definition and estimation

The IF of a nonstationary signal shows how its frequency content changes over time. Following (2), the definition of IF $f_z[n]$ is based on the derivative of the IP over time:

$$f_z[n] = F_s \frac{\varphi_z[n] - \varphi_z[n-1]}{2\pi}, \tag{3}$$

where F_s is the sampling frequency. Several methods have been suggested to estimate the IF of monocomponent and/or multicomponent nonstationary signals [25–29]. In [30], a new form of the Fourier transform and the local polynomial periodogram are developed for local polynomial approximation of the time-varying phase. The ICI (intersection of confidence intervals)-based methods utilize a nonparametric IF estimation approach to make a trade-off between bias and variance of the estimated IF [2,28,29]. Also, IF estimation using the properties of TFDs including adaptive short-time Fourier transform [31], QTFDs [32], T-class of TFDs [33], polynomial WVDs (PWVDs) [34,35] and complex-time distributions (CTDs) [36,37] have received a lot of attention. A detailed review on IF estimation algorithms can be found in [25–27]. Brief details are given below. In this study, we utilize three TFD-based IF estimators as well as a delay demodulator to extract the IF laws of monocomponent signals. The IF is also estimated using the phase derivative of the analytic associate defined as (3).

2.2.1. Phase derivative of the analytic associate

The most straightforward way of extracting the IF is taking the derivative of the IP. To this end, the underlying signal is converted into its analytic associate using the Hilbert transform according to (2). Then, the phase angles are corrected using an unwrapping method to produce smoother IP traces. In this study, we used the MATLAB command *unwrap* to smooth the IP by adding multiples of $\pm 2\pi$ to the absolute jumps between successive points greater than or equal to π radians. Finally, the IF is obtained based on its original definition as the derivative of the IP given by (3).

2.2.2. TFD-based IF estimation

The first order moment of a digitized QTFD $\rho_z[n,k]$ with respect to frequency (aka the normalized linear moment IF estimator) is defined as [38]:

$$f_z[n] = \frac{F_s}{2M} \frac{\sum_{k=0}^{M-1} k \rho_z[n,k]}{\sum_{k=0}^{M-1} \rho_z[n,k]}. \tag{4}$$

Based on (4), $f_z[n]$ is the weighted mean frequency of the signal.

2.2.3. Real base-band delay demodulator (RBBDD)

In order to estimate the IF of the analytic associate $z_s[n]$ in this method [39], it is first normalized, i.e.:

$$z_{sn}[n] = \frac{z_s[n]}{\lvert z_s[n]\rvert} = z_r[n] + jz_i[n]. \tag{5}$$

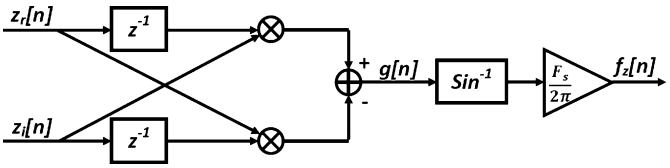

Fig. 1. Block diagram of the real base-band delay demodulator.

The block diagram depicted in Fig. 1 is then used to extract the IF. The term $g[n]$ in Fig. 1 can be written as:

$$g[n] = \sin\big(\varphi_z[n]\big)\cos\big(\varphi_z[n-1]\big) - \sin\big(\varphi_z[n-1]\big)\cos\big(\varphi_z[n]\big) = \sin\big(\varphi_z[n] - \varphi_z[n-1]\big) \tag{6}$$

which results in the estimated IF having the general form of (3). It is worth mentioning that although this approach results in the same estimation for the IF as the first derivative, it has the advantage of not requiring the computation of the IP of the signal which can be problematic.

2.3. Monocomponent signals vs. multicomponent signals: necessity of signal decomposition for IF estimation

In practice, the vast majority of real signals are multicomponent. In such cases, $\varphi_z[n]$ in (2) will represent an ambiguous or meaningless weighted squared average of the phases corresponding to different components of the signal [10]. Therefore, the definition of IF in (3), based on the Hilbert transform, becomes useless [40]. Filtering in the frequency domain to isolate T-F components may lead to distortion of the waveforms. Therefore, IF estimation of the nonstationary signals requires a separation of the T-F components prior to estimating the IFs [10]. Although there are other methods in the literature to deal with the multicomponent nonstationary signals (e.g., see [41,42]), we adapt EMD for decomposing the signals in our proposed approach. In contrast to most existing methods, the EMD follows a fully data-driven scheme which does not need any a priori knowledge about the signal. The technique is an adaptive method which breaks down a nonstationary and nonlinear signal into its intrinsic mode functions (IMFs) [43]. Each IMF is a monocomponent signal which generates no interference in a QTFD [44]. In other words, the IMFs represent simple oscillatory modes with time-varying amplitude and frequency:

$$s[n] = \sum_{k=1}^{M} IMF_k[n] + r[n], \tag{7}$$

where $s[n]$ is a real-valued multicomponent signal with M components and $r[n]$ is the residue [40,43]. By applying the Hilbert transform to (7), the analytic associate $z_s[n]$ can then be expressed as [40,43]:

$$z_s[n] = \sum_{k=1}^{M} a_z^{(k)}[n] e^{j\varphi_z^{(k)}[n]}, \tag{8}$$

where $a_z^{(k)}$ and $\varphi_z^{(k)}$ are respectively the instantaneous amplitude and phase associated with of the kth IMF. Each IMF contains a limited frequency content of its original signal, as EMD acts basically as a dyadic filter bank [45]. It turns out that with adequate length, an IMF satisfies the assumption of an asymptotic signal. The EMD process is described in Appendix A.

3. Formulation and assessment of phase synchrony

3.1. Bivariate phase synchrony

Let $z_x[n]$ and $z_y[n]$ be the analytic associates of two one-dimensional stochastic real-valued signals $x[n]$ and $y[n]$, respectively; that is:

$$z_x[n] = x[n] + j\tilde{x}[n] = a_x[n]e^{j\varphi_x[n]}, \tag{9}$$

$$z_y[n] = y[n] + j\tilde{y}[n] = a_y[n]e^{j\varphi_y[n]}, \tag{10}$$

where $\tilde{x}[n]$ and $\tilde{y}[n]$ are the Hilbert transforms of $x[n]$ and $y[n]$, respectively. The original signals are assumed to be asymptotic signals [2]. The two signals $x[n]$ and $y[n]$ are said to be *phase-locked of order* $P_x{:}P_y$ if [3]:

$$\Delta\varphi_{x,y}[n] = P_x\varphi_x[n] - P_y\varphi_y[n] = \text{const.} \tag{11}$$

Such a strict condition is rarely satisfied for real-life signals. Therefore, this condition is often replaced with a more relaxed condition called *phase entrainment* condition expressed by [3]:

$$\big|P_x\varphi_x[n] - P_y\varphi_y[n]\big| < \text{const.} \tag{12}$$

The ratio P_x/P_y is assumed to be rational. In the case of discrete signals and for the case $P_x = P_y = 1$ (phase locking of order 1:1), the phase synchrony measure is given by [3]:

$$R = \left|\frac{1}{N}\sum_{k=1}^{N-1} e^{j(\varphi_x[n]-\varphi_y[n])}\right|, \tag{13}$$

where N is the length of the two signals in samples. The measure R is often referred to as *mean phase coherence* (*MPC*) or *phase-locking value* (*PLV*) [3,4]. The measure R varies between 0 and 1, while the small phase difference between two signals makes R close to 1.

3.2. Generalized phase synchrony (GePS)

The classical definition of phase synchrony for bivariate signals can be extended to multivariate signals using the concept of cointegration [46].

3.2.1. Cointegration concept

A one-dimensional stochastic process is said to be *integrated of order d* ($I(d)$) if the reverse characteristic polynomial of its fitted multivariate autoregressive (MVAR) model has d roots on the unit circle in the z-complex plane [11]. The $I(d)$ process is unstable, but it can be converted into a stable one ($I(0)$) by d times differentiation [11]. Two or more integrated signals can be in a long-run relation with each other if there is a linear combination of these signals that results in a stationary process [11]. In such case, the underlying signals are called *cointegrated* signals with cointegration rank r. The parameter r represents the number of cointegrating relationships among the signals. Multivariate Johansen test can be used to determine the cointegration rank and cointegrating coefficients across multivariate integrated processes [11,47]. For more details about the Johansen test, refer to Appendix B.

3.2.2. Phase synchrony assessment based on the cointegration concept

Two signals $x_1[n]$ and $x_2[n]$ are said to be in a *generalized phase synchronous relationship* if their phases satisfy the following condition [11,12]:

$$\exists c_1, c_2{:}\ c_1\varphi_1[n] + c_2\varphi_2[n] = e[n], \tag{14}$$

where $e[n]$ is a normally distributed stationary stochastic process with finite second order moment and c_1 and c_2 are real-valued

numbers. The relation presented in (14) reflects a cointegrating relationship between two phase signals $\varphi_1[n]$ and $\varphi_2[n]$. Given $\varphi_x[n] = [\varphi_1[n], \ldots, \varphi_K[n]]$ as the multivariate phase signal associated with $x[n] = [x_1[n], \ldots, x_K[n]]^T$ a multivariate real-valued signal with K variables, such relationship can be generalized to a multivariate cointegrating relationship among K phase signals as follows:

$$\exists c_1, \ldots, c_K\colon\ c_1\varphi_1[n] + c_2\varphi_2[n] + \cdots + c_K\varphi_K[n] = e[n]. \tag{15}$$

The Hilbert transform is used to obtain the phase of each signal component $x_i[n]$ separately. If the multivariate instantaneous phase signal $\varphi_x[n]$ is integrated of order r, there are r stationary linear relationships within $\varphi_x[n]$ and the signal $x[n]$ is said to be in *generalized phase synchrony of rank r* [11,12]. A higher rank implies a larger number of phase signals are involved in relationships and therefore, higher synchrony within channels. Based on (15), cointegrating coefficients $c_1, \ldots, c_K$ and the cointegration rank r ($0 \leqslant r \leqslant K$) are estimated using the multivariate Johansen test [47].

4. Proposed IF-based generalized phase synchrony quantification

The phase angle $\varphi_z[n]$ in (2) usually exceeds the range $-\pi$ to π, which results in unpredicted $\pm 2\pi$ jumps between some consecutive phase values [48]. This problem is due to the stochastic nature of the sampled signal where the angular distance between two successive samples may be multiples of 2π. Although one may use the unwrapping methods to deal with the problem, we propose the use of the IF laws of the signals instead of their IPs to skip the issue. We take advantage of the direct relationship between the IP and the IF to extract the cointegrating relations within phase signals by simply differentiating (15) with respect to time. A measure is then defined to quantify the level of interaction.

4.1. Interpretation of the IF-based GePS

Suppose $x[n]$ and $y[n]$ are two periodic signals, phase-locked of order $P_x : P_y$ where both P_x and P_y are integers. Let the two signals start from a similar point on the time axis. If the phase-locking ratio is rational, it implies that the two signals will cross each other periodically at the same initial common value and this period is related to the least common multiple (LCM) between P_x and P_y. Therefore, the rational phase-locking order is associated with an intuitive physical meaning for periodic signals. In contrast, the two periodic signals never reach the same point with passing time in the case of irrational P_x/P_y.

Explanation of phase synchrony for non-periodic signals is not such straightforward. It becomes even more difficult for nonstationary signals which by definition cannot be periodic. In this case, the concept of frequency flows [10] in the T-F domain may help to clarify the issue. The notion of phase synchrony in (12) is strictly equivalent to the concept of frequency synchrony through the following formulation [10]:

$$\Delta\varphi_{x,y}[n] = P_x\varphi_x[n] - P_y\varphi_y[n] \approx \text{const} \tag{16}$$

which leads to

$$\begin{aligned}\frac{1}{2\pi}\,diff\big(\Delta\varphi_{x,y}[n]\big) &= \frac{P_x}{2\pi}\,diff\big(\Delta\varphi_x[n]\big) - \frac{P_y}{2\pi}\,diff\big(\Delta\varphi_y[n]\big)\\ &= P_x f_x[n] - P_y f_y[n] \approx 0\end{aligned}$$

$$\Rightarrow \quad f_x[n] \approx \frac{P_y}{P_x} f_y[n]. \tag{17}$$

This means that the two signals have similar IF shapes. The condition becomes equality when $P_x = P_y$. From this perspective, the concepts of phase synchrony and IF are connected [2,10].

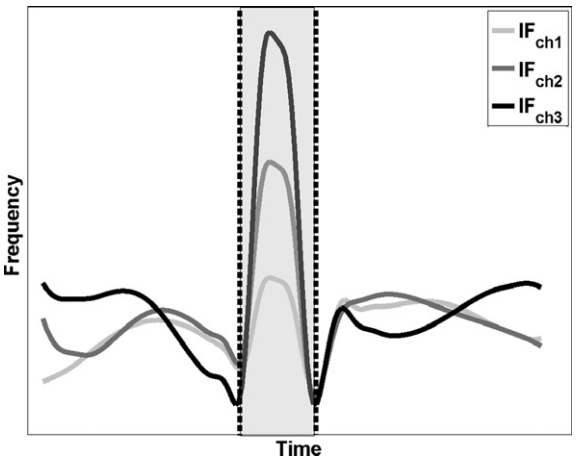

Fig. 2. An example of generalized phase synchrony within a three-channel signal (curves show IF ridges in the T-F domain. Shadowed area illustrates the phase-locking time period).

If two signals have similar IF laws during a time interval, they are phase-locked of order 1:1 over that time period [10]. Consequently, a linear relationship between two IFs with rational gain (P_x/P_y) implies phase locking of order P_x:P_y. Such a definition cannot explain GePS in the case where the linear relationships between phase signals can be irrational. Therefore, the following interpretation is proposed for generalized phase synchronization based on the concept of cointegration [12]:

For a multi-channel nonstationary signal, if there is a linear relationship between the IF laws of a subgroup of channels during a reasonably long time period, they are said to be generally phase synchronized over that time period.

In this case, there is no reason for the coefficients to be integer as the notion of phase-locked may not in general apply. Fig. 2 illustrates an example of GePS within the IFs of three channels. As the figure shows, there is *a linear relationship* (see the shadowed area) for all three IF laws during the shadowed time interval. Such linear combination defines a generalized phase locking between channels. Note that the new explanation reduces to the classical definition of phase synchrony for rational phase-locking orders.

4.2. Implementation of the proposed approach

The proposed procedure of GePS assessment for a nonstationary K-dimensional signal $x[n]$ is fully described by the following steps:

1. Each channel $x_i[n]$ $(i = 1, \ldots, K)$ is decomposed into Q IMFs $g_{x_i}^{(q)}[n]$ $(q = 1, \ldots, Q)$ using the EMD. The parameter Q can be estimated by the EMD stoppage criteria [40] as $Q = \min_i Q_i$ $(i = 1, \ldots, K)$ where Q_i is the number of IMFs in the ith channel. It is then kept the same for all channels.
2. The analytic associate of each IMF for the ith channel is obtained using the Hilbert transform, $z_i^{(q)}[n] = g_{x_i}^{(q)}[n] + jH(g_{x_i}^{(q)}[n])$ and its IP is extracted, $\varphi_{z_i}^{(q)}[n] = angle\{\frac{H(g_{x_i}^{(q)}[n])}{g_{x_i}^{(q)}[n]}\}$. The phases $\varphi_{z_i}^{(q)}[n]$ are then corrected using an unwrapping method [48] to suppress phase angle jumps between consecutive elements and produce smoother phase traces. The IF $f_{z_i}^{(q)}[n]$ are then extracted by taking the derivative of the unwrapped phase signals $\varphi_{z_i}^{(q)}[n]$. The IF $f_{z_i}^{(q)}[n]$ may also be estimated using other IF estimates that bypass the problem of phase ambiguity (see Section 2).

3. IFs of all channels at each decomposition level $f_z^{(q)} = [f_{z_i}^{(q)}, \ldots, f_{z_K}^{(q)}]$ are divided into non-overlapping time segments with adequate length. The minimum window length is determined based on the requirement of the MVAR parameter estimation where the length should be significantly larger than $K^2 p$ (p is the MVAR model order in the Johansen test) [49].
4. The Johansen method (maximum eigenvalues test) [11,47] is applied on each multivariate segment at the 99% confidence level and the linear relationships between IFs are extracted as follows:

$$\begin{cases} c_{11} f_{z_1}^{(q)}[n] + c_{12} f_{z_2}^{(q)}[n] + \cdots + c_{1K} f_{z_K}^{(q)}[n] = e_1^{(q)}[n], \\ c_{21} f_{z_1}^{(q)}[n] + c_{22} f_{z_2}^{(q)}[n] + \cdots + c_{2K} f_{z_K}^{(q)}[n] = e_2^{(q)}[n], \\ \vdots \\ c_{r^{(q)}1} f_{z_1}^{(q)}[n] + c_{r^{(q)}2} f_{z_2}^{(q)}[n] + \cdots + c_{r^{(q)}K} f_{z_K}^{(q)}[n] = e_{r^{(q)}}^{(q)}[n], \end{cases} \tag{18}$$

where $f_{z_i}^{(q)}[n]$ represents the ith segmented IF ($i = 1, \ldots, K$) of the qth IMF ($q = 1, \ldots, Q$), $r^{(q)}$ ($0 \leqslant r^{(q)} \leqslant K$) is the number of cointegrating relationships within the multivariate segment, c_{ki} ($k = 1, \ldots, r^{(q)}$) is the kth cointegrating coefficient of $f_{z_i}^{(q)}[n]$ and $e_k^{(q)}[n]$ is the stationary residual of the kth cointegrating relationship at the qth IMF.
5. The phase synchrony measure for each segment is defined as the normalized number of the cointegrating relationships $r^{(q)}$ over the IMF components:

$$\eta^{seg} = \frac{1}{Q.K} \sum_{q=1}^{Q} r^{(q)}. \tag{19}$$

This measure always takes values between 0 and 1 where 0 means no cointegrating relationship within phase signals and 1 implies complete phase cointegration within the multivariate segment.

4.3. Statistical analysis

The proposed method performance is evaluated using the receiver operating characteristic (ROC) curve to determine *sensitivity* and *specificity*. Suppose the multivariate signal $x[n]$ is divided into N segments with $N_{synch} \leqslant N$ segments present generalized phase synchrony. True positive rate (TPR), true negative rate (TNR), false positive rate (FPR) and false negative rate (FNR) of the method are defined as:

$$TPR = \frac{\text{No of segments correctly marked as synchronized}}{N_{synch}},$$

$$TNR = \frac{\text{No of segments correctly marked as synchronized}}{N - N_{synch}},$$

$$FPR = \frac{\text{No of segments correctly marked as synchronized}}{N_{synch}},$$

$$FNR = \frac{\text{No of segments correctly marked as synchronized}}{N - N_{synch}}.$$

The sensitivity and specificity of the method are then defined as follows:

$$Sensitivity = \frac{TPR}{TPR + FNR},$$

$$Specificity = \frac{TNR}{TNR + FPR}.$$

The ROC curve of the method is then obtained by plotting the sensitivity versus (1-specificity). The ROC also allows the calculation of the optimum threshold, where the maximum sensitivity meets the minimum FPR.

5. Results and discussion

In this section we evaluate the performance of the proposed method on both simulated and real newborn EEG signals using 5 different IF estimation methods, namely phase derivative of the analytic associate, three TFD-based IF estimators and RBBDD.

5.1. Simulated signals

In order to evaluate the performance of the proposed approach with different IF estimators for the nonstationary multivariate case, two 4-channel nonstationary signals with a length of 1000 seconds and unit amplitude at the sampling frequency of 100 Hz were simulated. For the asynchronous signal, the phase $\varphi_i[n]$ of each channel i was defined as an integrated process of order two. The phase $\varphi_i[n]$ was therefore obtained as the output of a linear shift-invariant system whose impulse response has two poles on the z-plane unit circle:

$$H(z) = \frac{1}{(1 - z^{-1})^2} \tag{20}$$

driven by a white noise process $w[n]$. The discrete form of the process in the time domain is therefore given by:

$$\varphi_i[n] = 2\varphi_i[n-1] - \varphi_i[n-2] + w[n], \quad 1 \leqslant i \leqslant 4,\ n = 1, \ldots, L, \tag{21}$$

where $L = 100\,000$ samples and $\varphi_i[1] = \varphi_i[2] = 0$. It implies that the IF laws are integrated processes of order one (one pole on the z-plane unit circle – random walk). In other words, there is no cointegrating relationship within the IFs or equivalently, no generalized phase synchrony within the channels. The asynchronous signal x^{asynch} was then defined as:

$$x^{asynch}[n] = real\{e^{j\varphi[n]}\}, \tag{22}$$

where $\varphi[n] = [\varphi_1[n], \ldots, \varphi_4[n]]$. A perfectly synchronous 4-channel signal with the same form of (22) was also simulated with random walk phase signals:

$$\varphi_i[n] = \varphi_i[n-1] + w[n], \quad 1 \leqslant i \leqslant 4,\ n = 1, \ldots, L, \tag{23}$$

where $\varphi_i[1] = 0$. It yields IFs with stationary trends with four cointegrating relationships. Both signals were divided into 4-sec segments and 100 segments were drawn out of the pool for each condition (synchrony/asynchrony). The dynamics of all phase signals was slowed artificially by a moving average process with the span of one second to magnify slow drift of the mean phase. Since the simulated signals are composed of multiple random frequency components, generalized phase synchrony can be observed within different intrinsic mode functions. Therefore, as described in Appendix A, an EMD sifting process was initially applied to decompose each channel of the segments into 5 IMFs. The proposed GePS measure was then extracted from the segments at each IMF, i.e. 5 measures for each segment. The final measure for the segment was obtained by taking the average over 5 values. The MVAR model order for the Johansen test was set to 10 during the process.

Four IF estimation methods (RBBDD, SPEC, MBD and CWD), along with the classical procedure of obtaining IF laws as the unwrapped phase derivative, were applied on the decomposed synchronous and asynchronous simulated signals. Fig. 3 illustrates the ROC curves of the synchrony/asynchrony detection method associated with the IF estimators.

In order to gain more insight into the performance of the IF estimators, the areas under the curve (AUCs) were computed for the ROC curves on the simulated signals. Table 2 summarizes the

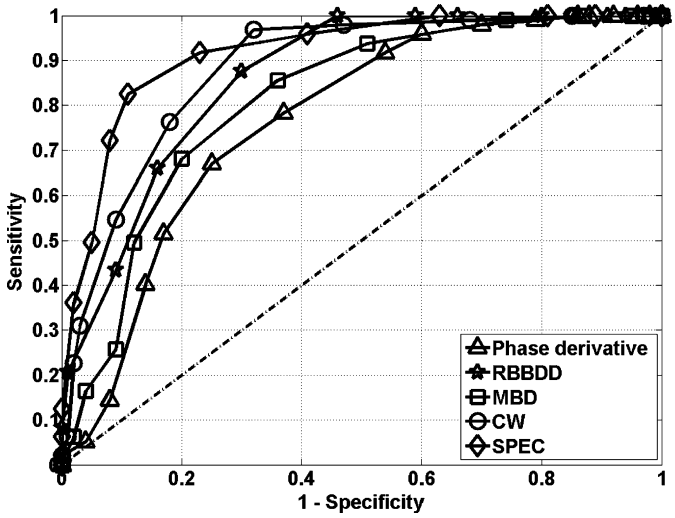

Fig. 3. ROC curves of the IF estimation methods used in this paper to extract generalized phase synchrony within the simulated signals.

Table 2
Area under curve for the ROC plots of Fig. 3.

IF estimator	AUC (%)
Phase derivative	79
RBBDD	85
CWD	88
MBD	82
SPEC	92

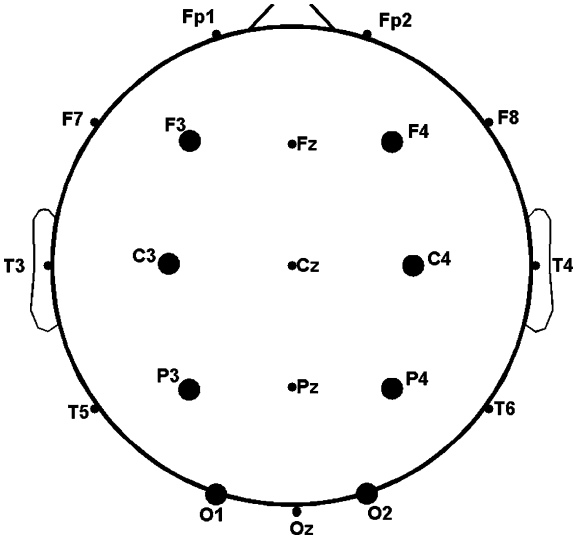

Fig. 4. Arrangement of the electrodes. Large circles illustrate the utilized electrodes.

AUC of the ROC plots in Fig. 3. As the results suggest, the CWD- and SPEC-based IF estimators showed the highest discrimination rate for estimating the GePS measure from the simulated signals.

The next section presents the GePS assessments with neonatal EEG signals in the presence and absence of seizure.

5.2. Newborn EEG analysis

5.2.1. Datasets, preprocessing and segmentation

Eight monopolar channels (F_3, F_4, C_3, C_4, P_3, P_4, O_1 and O_2) out of 14 channels recorded using the 10–20 standard [50] were selected from the EEG datasets of five newborns. Fig. 4 illustrates the arrangement of the electrodes. These electrodes were chosen according to the symmetrical combination of electrodes from left and right hemispheres in order to enable inter-hemispheric phase synchrony assessment. The data was recorded using a Medelec Profile system (Medelec, Oxford Instruments, Old Woking, UK) at 256 Hz sampling rate and marked for seizure by a pediatric neurologist from the Royal Children's Hospital, Brisbane, Australia. All signals were bandpass filtered within 0.5–30 Hz using an FIR filter of order 100. The filtered signals were inspected visually to remove highly artifactual segments. Artifact free intervals were then segmented into 4-sec windows. In this study, 100 non-overlapping ictal segments and 100 non-overlapping interictal segments were extracted randomly from 27 min of artifact-free seizure signals and 39 min of artifact-free non-seizure signals obtained from 5 subjects. The window length (1024 samples) was chosen to be larger than $K^2 p$ where p is the MVAR model order for the Johansen test (here, $p \leqslant 6$) and K is the number of channels (here, $K = 8$).

5.2.2. Significant increment of the GePS measure during the seizure periods

The procedure described in Section 3 was applied on each 8-channel (4 left and 4 right) newborn EEG segment in order to analyze the generalized phase synchronization within both seizure and non-seizure groups. Fig. 5 illustrates the Modified-B distributions ($\beta = 0.01$, $L_{lag} = N/4$) and time traces of 5 IMFs extracted from 2 adjacent left-right electrodes (F_3 and F_4) for a random seizure segment. The IFs of each multi-channel segment at each decomposition level (each IMF) are analyzed by the Johansen test. The cointegration ranks of the IMFs are then utilized for calculating the GePS measure of the underlying segment using (19). A vertical frequency shift can be observed between each two successive rows in Fig. 5. This observation reflects the nature of the EMD sifting process as a dyadic filter bank [45]. As the figure suggests, the IMFs can be roughly linked to the EEG frequency bands: IMF5 covers the δ band (up to 5 Hz), IMF4 covers the δ and θ bands (up to 10 Hz), IMF3 mostly covers the θ and α bands (5–15 Hz), IMF2 mostly covers the α and β bands (10–20 Hz) and IMF1 mostly covers the β and γ bands (above 20 Hz).

In order to evaluate the performance of the IF estimators for quantifying newborn EEG generalized phase synchrony, five methods were employed. Fig. 6 exhibits the ROC curves of the IF estimators on the seizure/non-seizure EEG segments. As the figure implies, the sensitivity is significantly higher than the false alarm (1-specificity) for all estimators. It indicates increased GePS measures within the seizure segments compared to the non-seizure segments.

Table 3 contains the AUC values associated with the ROC curves in Fig. 6. From the table, it becomes clear that most estimators are significantly different from the chance level (50%). However, the AUC values remain lower than what was obtained for the simulated signals (see Table 2). Unlike the simulated data analysis, performance of the TFD-based IF estimators on the EEG data is lower than the phase derivative and RBBDD.

A two-sample t-test was conducted on the newborn EEG results to evaluate the null hypothesis that two groups of GePS values estimated by the unwrapped phase derivative estimator are independent random samples with equal means against the alternative that the means are not equal. The resultant p-value at the 1% significance level was 1.18×10^{-8} implying that the mean GePS values of the seizure group are significantly higher than the non-seizure group ($GePS_{seiz} = 0.46 \pm 0.14$, $GePS_{nonseiz} = 0.36 \pm 0.08$).

5.3. Discussion

The results presented in the previous section show differences between the performances of IF estimators used in the simulated signals and newborn EEG. We have demonstrated that the

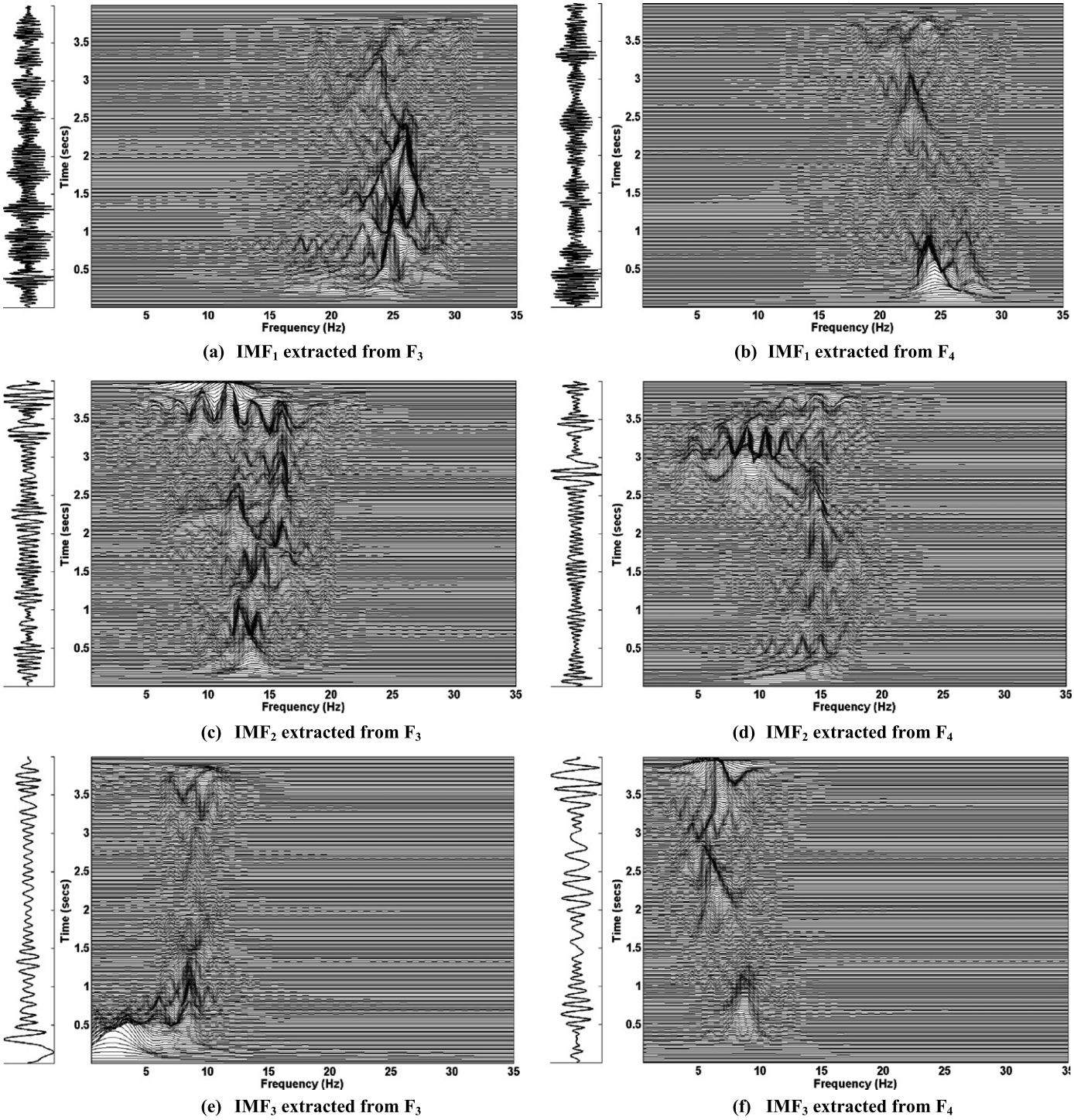

Fig. 5. Modified-B distributions ($\beta = 0.01$, $L_{lag} = N/4$) and time traces of the IMFs at five decomposition levels extracted from two adjacent left–right electrodes (F_3 and F_4).

EMD sifting process can be used in estimating the GePS measure to break down multi-component signals into monocomponent signals, containing relevant information for evaluation of the cointegrating relationships within the multivariate datasets. EMD provides a clearer physical interpretation for synchronization between broadband signals, as it does for the EEG datasets. This is of high importance, as the role of the selected frequency band is always crucial for EEG analysis applications. The IMFs extracted from newborn EEG can be roughly linked to the well-defined EEG frequency bands. The results indicate that the GePS assessment proposed in this paper can be considered as a global evaluation of phase synchrony over all channels and all frequencies in a typical multi-channel newborn EEG signal. From this point of view, the choice of keeping a constant number of IMFs (here, five) during the whole EEG analysis is compatible with the nature of EEG signals. For the GePS measures derived from synchronization between simulated signals, maximum discrimination rates of 92% and 88% were obtained for the SPEC- and CWD-based IF estimators, respectively. The highest rates for newborn EEG signals were 75% and 71% associated with the phase derivative and RBBDD IF estimators, respectively. Unlike the simulations, the performance of TFD-based IF estimators on the newborn EEG data was lower than

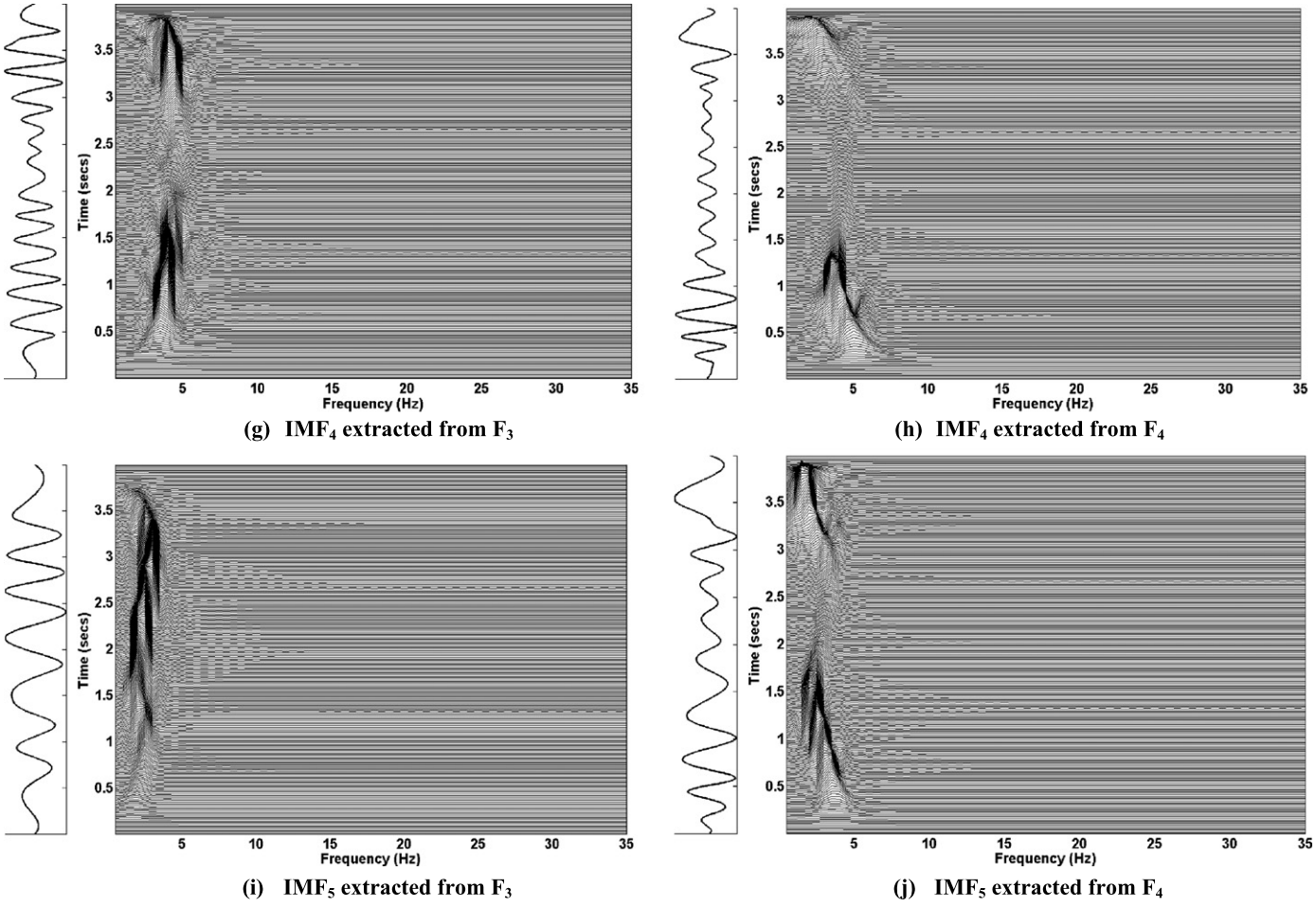

(g) IMF_4 extracted from F_3 (h) IMF_4 extracted from F_4

(i) IMF_5 extracted from F_3 (j) IMF_5 extracted from F_4

Fig. 5. (*continued*)

Table 3
Area under curve for the ROC plots of Fig. 6.

IF estimator	AUC (%)
Phase derivative	75
RBBDD	71
CWD	65
MBD	67
SPEC	62

the phase derivative estimator and the RBBDD method. This observation may imply that the TFD-based IF estimators are more vulnerable to the unknown factors (which will remain in the real EEG signals after pre-processing) compared to the phase derivative and RBBDD. Higher performance of the phase derivative estimator for newborn EEG analysis also suggests that the IMFs extracted from the EEG channels satisfy the requirements of the asymptotic signals [2].

The statistical results also suggest that there is a constant inter-hemispheric connectivity within the newborn brain during the interictal periods as all of the $GePS_{nonseiz}$ values are greater than zero. This is consistent with fMRI-based studies suggesting stable low-frequency, spontaneous fluctuations within the newborn brain during resting-state conditions, termed resting-state networks [51,52]. This study also suggests that the inter-hemispheric connectivity increases during seizure periods in terms of the GePS. This is in agreement with previous neonatal EEG studies where EEG channels are more synchronized within the seizure periods than the non-seizure intervals [53].

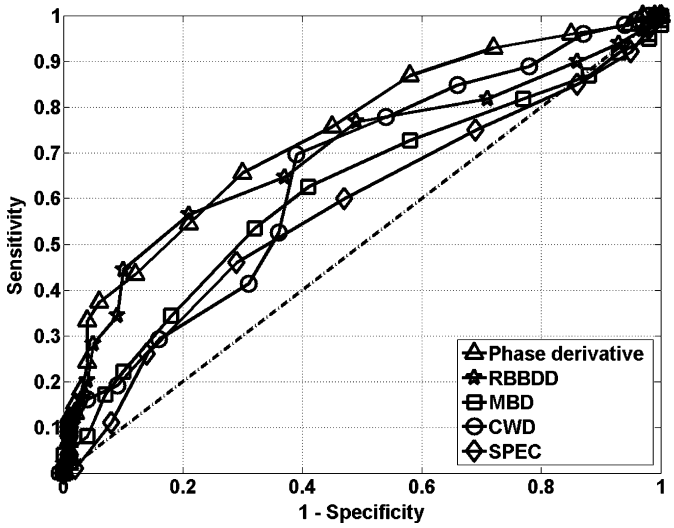

Fig. 6. ROC curves of the IF estimation methods used in this paper to extract GePS within the seizure/non-seizure EEG segments.

The effect of EEG montage is another important factor which needs to be investigated in all EEG phase synchrony assessments. While we have used a monopolar montage for this study, other montages such as bipolar, average reference and Laplacian montages may give different results. In addition, it is worth exploring the effect of the number of electrodes in each group on the GePS measure. One, however, needs to be careful about selecting

the number of electrodes in EEG connectivity studies including phase synchrony assessment, as highly dense arrangement of the electrodes may increase the interfering effect of volume conduction between neighboring electrodes and affect the connectivity analysis results. Therefore, the effect of volume conduction needs to be explored in future work to assess its impact on the new measure of synchrony.

The ratio of synchronous time periods in the whole newborn EEG signal can be used as an index of newborn brain asynchrony. Such a single number as a representative of asynchronous bursts within a long newborn EEG recording may be used as a qualitative measure of EEG inter-hemispheric asynchrony. This could provide an accurate quantitative measure of asynchrony in the neonatal EEG, and thereby significantly improves the current way of providing only a qualitative description of synchrony/asynchrony from the newborn EEG. Such an objective tool is required to supplement the highly subjective, visual assessment of EEG (see also [54]).

6. Conclusion

This study establishes the relevance of the GePS measure for quantifying the global phase synchronization within multivariate nonstationary signals such as newborn EEG. A novel framework for GePS assessment within nonstationary multi-channel signals has been described based on IP/IF estimation in the time-frequency (T-F) domain. The approach has also been evaluated using different T-F methods to optimize its application to newborn EEG seizure detection. The significance of the proposed scheme is demonstrated by the finding that during seizure activity, greater synchrony is observed within multi-channel EEG signal. A statistical analysis of the results obtained suggests that the GePS increases significantly during the ictal periods. This is in agreement with previous neonatal EEG studies where EEG channels were more synchronized during ictal periods than interictal periods [55]. The promising simulation results suggest the SPEC- and CWD-based IF estimators as the most efficient IF estimators for GePS assessment. The TFD-based estimators, however, have lower performance on the newborn EEG datasets compared with the phase derivative estimator and the RBBDD method. The measure may also be utilized as a multivariate EEG feature for newborn EEG seizure detection. However, its discriminatory ability needs to be further analyzed and compared with the other existing newborn seizure detection methods. Also, the concept of generalized phase synchrony within the newborn brain calls for a more robust statistical study with larger populations. Unlike classical phase synchrony measures, the proposed measure deals with the generalized phase synchrony in cases where the phase-locking ratio is not rational. This allows a more flexible view of synchronous cycles within the nonstationary multi-channel signals. The statistical distribution of the GePS measure associated with the interictal (non-seizure) EEG signals of two hemispheres lies always above the zero level suggesting that there may be stable low-frequency and spontaneous fluctuations within the newborn brain. The proposed framework may help quantifying the inter-hemispheric functional connectivity within multi-channel newborn EEG signals. Future work will concentrate on improving the temporal resolution of the proposed approach, utilizing multi-component IF estimation techniques [41,42], and recruiting more subjects to support the statistical analysis and quantifying other newborn EEG abnormalities such as EEG asymmetry/asynchrony in preterm babies using the proposed approach. The findings of increased synchrony in seizure EEG and variable synchrony in non-seizure periods warrant exploration of the approach in a range of newborn neurological disorders where biomarkers and prognostic indicators are essential to improving management for these babies.

Acknowledgments

This publication was made possible by a grant from the Qatar National Research Fund under its National Priorities Research Program award number NPRP 09-465-2-174. The authors also thank Dr. Christopher Burke for marking seizure periods in the newborn EEG recordings.

Appendix A. Empirical mode decomposition (EMD)

We used the following procedure to derive the EMD process [9,40,43] in this study:

1. Let $\tilde{s}[n] = r_i[n]$, $r_1[n] = s[n]$, $i = 1, 2, 3, \ldots$.
2. Identify all the local maxima and minima of $\tilde{s}[n]$.
3. Connect all the local maxima together and all the local minima together by an interpolation method (e.g., spline) to obtain the upper envelope $e_{\max}[n]$ and the lower envelope $e_{\min}[n]$.
4. Update $\tilde{s}[n]$ as $\tilde{s}[n] = \tilde{s}[n] - 0.5(e_{\min}[n] + e_{\max}[n])$ and go to step 2.
5. Repeat steps 2–4 until a stoppage criterion is satisfied. $\tilde{s}[n]$ will then become an IMF.
6. Separate the IMF $h[n]$ from the rest of the data by $r_{i+1}[n] = s[n] - \tilde{s}[n]$. The residue $r_{i+1}[n]$ is then treated as the updated signal $s[n]$ and fed into the sifting process again (steps 1–5).

The process is repeated until no more IMFs can be extracted, in other words, the residue becomes a monotonic function. Other predetermined criteria such as thresholding on the energy of the residue can also be used [40].

Appendix B. Multivariate Johansen test

The Johansen test is a procedure for testing the cointegrating relationships of several integrated processes of order zero or one [44]. Since the test evaluates more than one cointegrating relationship within the time series, it is applicable for multivariate signals such as multi-channel EEG. The starting point of the test in this study is from an N-dimensional IF $f_z[n] \in \Re^{N\times 1}$ as a multivariate MVAR model of order p given by [11,55]:

$$f_z[n] = \mu + \sum_{r=1}^{p} A_r f_z[n-r] + \varepsilon[n], \tag{24}$$

where $A_r \in \Re^{N\times N}$ is the MVAR coefficient matrix at delay r, $\varepsilon[n] \in \Re^{N\times 1}$ is the input white noise of the model and $\mu \in \Re^{N\times 1}$ is a constant term. The assumption here is that the variables of $f_z[n]$ are integrated processes of either order one ($I(1)$) or order zero ($I(0)$ or a stationary process). The MVAR model described in (24) can be re-written in terms of the differences between its successive delayed values as:

$$\Delta f_z[n] = -\Pi f_z[n-1] + \sum_{r=1}^{p-1} \Gamma_r \Delta f_z[n-r] + \varepsilon[n], \tag{25}$$

where

$$\Pi = I - A_1 - \cdots - A_p, \tag{26}$$

$$\Gamma_r = -\sum_{j=r+1}^{p} A_j \tag{27}$$

and $\Delta f_z[n-i] = f_z[n-i] - f_z[n-i-1]$ [11,55]. Such transformed version of the MVAR models is called *vector error correlation model* (*VECM*). If r is the rank of the coefficient matrix $\Pi (r < N)$, then there exist two full-rank matrices α and β ($\alpha, \beta \in \Re^{r\times N}$) such

that $\beta^T f_z[n]$ is stationary and $\Pi = \alpha\beta^T$. The rank r determines the number of coefficient relationships between the dimensions of $f_z[n]$. Cointegrating vectors of the process are also obtained from the columns of β. Based on the maximum likelihood estimation of β for a given r, the Johansen method performs two different likelihood ratio tests: *the trace test* and *the maximum eigenvalue test*. The former one tests a hypothesis H_0 against an alternative H_1, where

H_0: there are r cointegrating relationships between variables,
H_1: there are k cointegrating relationships between variables.

For the latter one, the null and alternative hypotheses are defined as:

H_0: there are r cointegrating relationships between variables,
H_1: there are $r+1$ cointegrating relationships between variables.

In the special case of $r = N$ (Π has full-rank), all variables of the process are stationary and there is no conintegrating relationship between them [55]. In this study, the MATLAB implementation of the multivariate Johansen test provided in the Econometrics toolbox [56] was used.

References

[1] K.J. Blinowska, R. Kusacute, M. Kaminacuteski, Granger causality and information flow in multivariate processes, Phys. Rev. E 70 (2004) 050902(R).
[2] B. Boashash (Ed.), Time Frequency Signal Analysis and Processing: A Comprehensive Reference, Elsevier, Amsterdam, Boston, 2003.
[3] F. Mormann, K. Lehnertz, P. David, C.E. Elger, Mean phase coherence as a measure for phase synchronization and its application to the EEG of epilepsy patients, Physica D 144 (2000) 358–369.
[4] J.P. Lachaux, E. Rodriguez, J. Martinerie, F.J. Varela, Measuring phase synchrony in brain signals, Hum. Brain Mapp. 8 (1999) 194–208.
[5] M.G. Rosenblum, A.S. Pikovsky, Detecting direction of coupling in interacting oscillators, Phys. Rev. E 64 (2001) 045202.
[6] M.G. Rosenblum, L. Cimponeriu, A. Bezerianos, A. Patzak, R. Mrowka, Identification of coupling direction: application to cardiorespiratory interaction, Phys. Rev. E 65 (2002) 041909.
[7] T. Koenig, D. Lehmann, N. Saito, T. Kuginuki, T. Kinoshita, M. Koukkou, Decreased functional connectivity of EEG theta-frequency activity in first-episode, neuroleptic-naïve patients with schizophrenia: preliminary results, Schizophr. Res. 50 (2001) 55–60.
[8] D. Looney, C. Park, P. Kidmose, M. Ungstrup, D.P. Mandic, Measuring phase synchrony using complex extensions of EMD, in: IEEE 15th Workshop on Stat. Signal Process., Cardiff, UK, 2009, pp. 49–52.
[9] A.Y. Mutlu, S. Aviyente, Multivariate empirical mode decomposition for quantifying multivariate phase synchronization, EURASIP J. Adv. Sig. Process. 2011 (2011) 61517.
[10] D. Rudrauf, A. Douiri, C. Kovach, J.P. Lachaux, D. Cosmelli, M. Chavez, C. Adam, B. Renault, J. Martinerie, M. Le van Quyen, Frequency flows and the time–frequency dynamics of multivariate phase synchronization in brain signals, Neuroimage 31 (2006) 209–227.
[11] A.R. Kammerdiner, P.M. Pardalo, Analysis of multichannel EEG recordings based on generalized phase synchronization and cointegrated VAR, in: W. Chaovalitwongse, P.M. Pardalos, P. Xanthopoulos (Eds.), J. Comput. Neurosci. 38 (2010) 317–339.
[12] A. Omidvarnia, B. Boashash, G. Azemi, P. Colditz, V. Vanhatalo, Generalised phase synchrony within multivariate signals: an emerging concept in time–frequency analysis, in: IEEE 37th Intl. Conf. on Acoustics, Speech, and Signal Process., Kyoto, Japan, 2012.
[13] A. Omidvarnia, S. Vanhatalo, M. Mesbah, G. Azemi, P. Colditz, B. Boashash, Generalized mean phase coherence for asynchrony abnormality detection in multichannel newborn EEG, in: IEEE 11th Intl. Conf. on Inform. Sci., Signal Process. and Their Applications, Montreal, Canada, 2012, pp. 274–279.
[14] A.D. Bakhshi, M.A. Maud, K.M. Aamir, A. Loan, Cardiac arrhythmia detection using instantaneous frequency estimation of ECG signals, in: International Conference on Information and Emerging Technologies Karachi, Pakistan, 2010, pp. 1–5.
[15] Q. Lunji, L. Gang, Representation of ECG signals based on the instantaneous frequency estimation, in: 3rd Intl. Conf. on Signal Process., Beijing, China, 1996, pp. 1731–1734.
[16] I. Orović, S. Stanković, T. Thayaparan, L.J. Stanković, Multiwindow S-method for instantaneous frequency estimation and its application in radar signal analysis, IET Signal Process. 4 (2010) 363–370.
[17] F. Berizzi, G. Pinelli, Maximum-likelihood ISAR image autofocusing technique based on instantaneous frequency estimation, IEE Proc. Radar Sonar Navigat. 144 (1997) 284–292.
[18] L. Xue Mei, T. Ran, L. Yan Lei, SAR autofocus based on the instantaneous frequency estimation, in: 2nd Asian–Pacific Conf. on Synth. Aperture Radar, China, 2009, pp. 417–420.
[19] S.S. Abeysekera, Instantaneous frequency estimation from FM signals and its use in continuous phase modulation receivers, in: 7th Intl. Conf. on Inform. Communic., and Signal Process., Macau, 2009, pp. 1–5.
[20] Y. Jiexiao, L. Kai Hua, L. Peng, A mobile RFID localization algorithm based on instantaneous frequency estimation, in: 6th Intl. Conf. on Comp, Sci. and Edu., Singapore, 2011, pp. 525–530.
[21] W.J. Williams, Reduced interference distributions: biological applications and interpretations, Proc. IEEE 84 (1996) 1264–1280.
[22] N. Stevenson, M. Mesbah, B. Boashash, Quadratic time–frequency distribution selection for seizure detection in the newborn, in: 30th Annual Intl. Conf. of the IEEE Eng. in Med. and Biol. Soci., Vancouver, BC, 2008, pp. 923–926.
[23] M.S. Khlif, M. Mesbah, B. Boashash, P. Colditz, Detection of neonatal seizure using multiple filters, in: 10th Intl. Conf. on Inform. Sci. Signal Process. and Their Applications, Kuala Lumpur, Malaysia, 2010, pp. 284–287.
[24] B. Boashash, V. Sucic, Resolution measure criteria for the objective assessment of the performance of quadratic time–frequency distributions, IEEE Trans. Signal Process. 51 (2003) 1253–1263.
[25] B. Boashash, Estimating and interpreting the instantaneous frequency of a signal. I. Fundamentals, Proc. IEEE 80 (1992) 520–538.
[26] B. Boashash, Estimating and interpreting the instantaneous frequency of a signal. II. Algorithms and applications, Proc. IEEE 80 (1992) 540–568.
[27] B. Boashash, P. O'Shea, M.J. Arnold, Algorithms for instantaneous frequency estimation: a comparative study, in: Adv. Sig. Process. Alg., Arch., and Implement., San Diego, CA, USA, 1990, pp. 126–148.
[28] I. Djurovic, L. Stankovic, Modification of the ICI rule-based IF estimator for high noise environments, IEEE Trans. Signal Process. 52 (2004) 2655–2661.
[29] J. Lerga, V. Sucic, Nonlinear IF estimation based on the pseudo WVD adapted using the improved sliding pairwise ICI rule, IEEE Signal Process. Lett. 16 (2009) 953–956.
[30] V. Katkovnik, Discrete-time local polynomial approximation of the instantaneous frequency, IEEE Trans. Signal Process. 46 (1998) 2626–2637.
[31] H.K. Kwok, D.L. Jones, Improved instantaneous frequency estimation using an adaptive short-time Fourier transform, IEEE Trans. Signal Process. 48 (2000) 2964–2972.
[32] Z.M. Hussain, B. Boashash, Adaptive instantaneous frequency estimation of multicomponent FM signals using quadratic time–frequency distributions, IEEE Trans. Signal Process. 50 (2002) 1866–1876.
[33] Z.M. Hussain, B. Boashash, The T-class of time–frequency distributions: time-only kernels with amplitude estimation, J. Franklin Inst. 343 (2006) 661–675.
[34] B. Barkat, B. Boashash, L.J. Stankovic, Adaptive window in the PWVD for the IF estimation of FM signals in additive Gaussian noise, in: IEEE Intl. Conf. on Acoustics, Speech, and Signal Process., vol. 3, 1999, pp. 1317–1320.
[35] B. Ristic, B. Boashash, Instantaneous frequency estimation of quadratic and cubic FM signals using the cross polynomial Wigner–Ville distribution, IEEE Trans. Signal Process. 44 (1996) 1549–1553.
[36] I. Orović, M. Orlandić, S. Stanković, Z. Uskoković, A virtual instrument for time–frequency analysis of signals with highly nonstationary instantaneous frequency, IEEE Trans. Instrum. Meas. 60 (2011) 791–803.
[37] I. Orovic, A. Draganic, S. Stankovic, E. Sejdic, A unified approach for the estimation of instantaneous frequency and its derivatives for nonstationary signals analysis, Presented at the: IEEE 11th Intl. Conf. on Inform. Sci., Signal Process. and Their Applications, Montreal, Canada, 2012.
[38] P.J. Kootsookos, B.C. Lovell, B. Boashash, A unified approach to the STFT, TFDs, and instantaneous frequency, IEEE Trans. Signal Process. 40 (1992) 1971–1982.
[39] E. Zandi, G. Azemi, Estimating the scattering distribution of the received signal in micro-cellular systems, in: 16th Euro. Signal Process. Conf., Lausanne, Switzerland, 2008.
[40] N.E. Huang, S.S.P. Huang, Introduction to the Hilbert–Huang transform and its related mathematical problems, in: Hilbert–Huang Transform and Its Applications, World Scientific Publishing Company, 2005, p. 324, Chap. 1.
[41] L. Rankine, M. Mesbah, B. Boashash, IF estimation for multicomponent signals using image processing techniques in the time–frequency domain, Signal Process. 87 (2007) 1234–1250.
[42] J. Lerga, V. Sucic, B. Boashash, An efficient algorithm for instantaneous frequency estimation of nonstationary multicomponent signals in low SNR, EURASIP J. Adv. Sig. Process. 2011 (2011) 725189.
[43] N.E. Huang, Z. Shen, S.R. Long, M.C. Wu, H.H. Shih, Q. Zheng, N.-C. Yen, C.C. Tung, H.H. Liu, The empirical mode decomposition and the Hilbert spectrum for nonlinear and nonstationary time series analysis, Proc. R. Soc. Lond. Ser. A Math. Phys. En. Sci. 454 (1998) 903–995.
[44] N.J. Stevenson, M. Mesbah, B. Boashash, Multiple-view time–frequency distribution based on the empirical mode decomposition, IET Signal Process. 4 (2010) 447–456.
[45] P. Flandrin, G. Rilling, P. Goncalves, Empirical mode decomposition as a filter bank, IEEE Signal Process. Lett. 11 (2004) 112–114.

[46] M.P. Murray, A drunk and her dog: an illustration of cointegration and error correction, Amer. Statist. 48 (1994) 37–39.
[47] S. Johansen, Estimation and hypothesis testing of cointegration vectors in Gaussian vector autoregressive models, Econometrica 59 (1991) 1551–1580.
[48] Z.N. Karam, Computation of the one-dimensional unwrapped phase, Master of Science in Electrical Engineering, Masters thesis, Massachusetts Institute of Technology, 2006.
[49] H. Hytti, R. Takalo, H. Ihalainen, Tutorial on multivariate autoregressive modelling, J. Clin. Monit. Comput. 20 (2006) 101–108.
[50] E. Niedermeyer, F. Lopes da Silva, Electroencephalography: Basic Principles, Clinical Applications, and Related Fields, 5th ed., Lippincott Williams & Wilkins, 2004.
[51] V. Doria, C.F. Beckmann, T. Arichi, N. Merchant, M. Groppo, F.E. Turkheimer, S.J. Counsell, M. Murgasova, P. Aljabar, R.G. Nunes, D.J. Larkman, G. Rees, A.D. Edwards, Emergence of resting state networks in the preterm human brain, Proc. Natl. Acad. Sci. USA 107 (2010) 20015–20020.
[52] P. Fransson, B. Skiöld, S. Horsch, A. Nordell, M. Blennow, H. Lagercrantz, U. Ãden, Resting-state networks in the infant brain, Proc. Natl. Acad. Sci. USA 104 (2007) 15531–15536.
[53] J. Altenburg, R.J. Vermeulen, R.L.M. Strijers, W.P.F. Fetter, C.J. Stam, Seizure detection in the neonatal EEG with synchronization likelihood, J. Clin. Neurophysiol. 114 (2003) 50–55.
[54] B.H. Walsh, D.M. Murray, G.B. Boylan, The use of conventional EEG for the assessment of hypoxic ischaemic encephalopathy in the newborn: a review, J. Clin. Neurophysiol. 122 (2011) 1284–1294.
[55] E. Hjalmarsson, P. Osterholm, Testing for cointegration using the Johansen methodology when variables are near-integrated, Intl. Monetary Fund, Western Hemisphere Division, 2007.
[56] J.P. LeSage, Econometrics Toolbox, MATLAB functions, available at http://www.spatial-econometrics.com.

Amir Omidvarnia received his B.Sc. and M.Sc. degrees from the Amirkabir University of Technology, Tehran and the University of Tehran, in 2002 and 2005, respectively, both in Biomedical Engineering. He is currently enrolled in a Ph.D. degree in Biomedical Engineering at the University of Queensland, Centre for Clinical Research supported by a UQ International Postgraduate Research Scholarship. His research interests are medical signal processing and time–frequency analysis.

Ghasem Azemi received his Ph.D. in Signal Processing from Queensland University of Technology, Brisbane, Australia, in 2004. He then joined the Department of Electrical Engineering, Razi University, Kermanshah, Iran as an Assistant Professor. Since 2009, he is with the Centre for Clinical Research, University of Queensland, Brisbane, Australia as a Research Fellow. His research interests are biomedical, and time–frequency signal processing.

Paul B. Colditz is a neonatal clinician (MBBS, FRACP, FRCPCH) with a Masters in Biomedical Engineering (University of New South Wales) and a PhD from Oxford University. His research aim is to improve neurodevelopmental outcomes for babies through studies involving basic science, brain imaging (MRI) and electrophysiology (EEG).

Boualem Boashash (IEEE Fellow '99') is a Scholar, Professor and Senior Academic Manager with experience in 5 leading Universities in France and Australia. He has published over 500 technical publications, including 100 journal publications covering Engineering, Applied Mathematics and Biomedicine. He pioneered the field of Time–Frequency Signal Processing for which he published the most comprehensive book and developed the earliest most powerful software package. Among many initiatives, he founded ISSPA, a leading conference since 1985. After a previous appointment in the UAE as Dean of Engineering, he moved to Qatar University as an Associate Dean, Academic, and then a Research Professor.